Clearing the FoG: Antifungal tolerance is a subpopulation effect that is distinct from resistance and is associated with persistent candidemia

Alexander Rosenberg[1*], Iuliana V. Ene[2*], Maayan Bibi[1], Shiri Zakin[1], Ella Shtifman Segal[1], Naomi Ziv[3], Alon M. Dahan[1], Arnaldo L. Colombo[4], Richard J. Bennett[2], Judith Berman[1**]

1. School of Molecular Cell Biology and Biotechnology, Tel Aviv University, Ramat Aviv Israel
2. Department of Molecular Microbiology and Immunology, Brown University, Providence, Rhode Island, USA
3. Department of Microbiology & Immunology, University of California, San Francisco, San Francisco, CA, USA
4. Department of Medicine, Federal University of São Paulo, São Paulo, Brazil

*Equal contributions

**Corresponding Author: judithberman11@gmail.com, +972-52-584-2031

Abstract

Drug susceptibility, defined by the minimal inhibitory concentration (MIC), often does not predict whether fungal infections will respond to therapy in the clinic. Tolerance at supra-MIC antifungal drug concentrations is rarely quantified and current clinical recommendations suggest it be ignored. Here, we measured and characterized drug-response variables that could influence the outcomes of fungal infections and be generalizable across major clades of *Candida albicans*, one of the most frequently isolated human fungal pathogens. We quantified antifungal tolerance as the fraction of growth (FoG) above the MIC and found that it is clearly distinct from susceptibility/resistance measured as MIC. Instead, tolerance is due to the slow growth of subpopulations of cells that overcome drug stress more efficiently than the rest of the population, and correlates inversely with the accumulation of intracellular drug. Importantly, many adjuvant drugs used together with fluconazole, a fungistatic drug, reduce tolerance without affecting resistance. These include inhibitors of major stress response hubs such as Hsp90, calcineurin, PKC1 and TOR. Accordingly, in an invertebrate infection model, adjuvant combination therapy was significantly more effective than fluconazole alone in treating highly tolerant isolates and did not improve the treatment of isolates with low tolerance levels. Furthermore, isolates recovered from immunocompetent patients with persistent candidemia displayed significantly higher tolerance than isolates that were readily cleared by fluconazole. Thus, tolerance correlates with the response to fluconazole therapy in patients and may help predict whether infections will respond to fluconazole alone. Similarly, measuring tolerance may provide a useful clinical parameter for choosing appropriate therapeutic strategies to overcome persistent clinical candidemia.

Introduction

A goal of antimicrobial susceptibility testing is to predict the clinical success or failure of antibiotic therapy. Some infections are recalcitrant to drug treatment due to 'resistance', which refers to microbial growth in the presence of drug concentrations that inhibit susceptible isolates[1,2]. Susceptibility is commonly measured as the Minimal Inhibitory Concentration (MIC) after 24 h of growth in the presence of drug[3,4]. Fungal infections generally follow the "90/60" rule for predicting therapeutic outcomes based on *in vitro* susceptibility testing: ~90% of susceptible isolates and 60% of resistant isolates respond to therapy[5-9]. This implies that infection outcomes are influenced by host factors as well as features of the pathogen that are not reflected by the MIC[10,11]. In effect, organisms that cause persistent infections, defined as those that are not cleared by a course of antifungal treatment, have similar susceptibilities to organisms that are readily cleared by a course of antifungal treatment[12]. Accordingly, it is important to identify measurable parameters that can contribute to disease severity.

Only four classes of antifungals are currently in clinical use, and resistance to azoles, including fluconazole (FLC), the most commonly administered antifungal against *Candida* species, is an increasing problem. Altered drug uptake/drug efflux and changes in ergosterol biosynthesis (the target for azole drugs)[13] are the major known mechanisms of azole resistance. Stress responses have been proposed as a third mechanism of antifungal resistance[14]. A broad range of small molecules enhance antifungal activity *in vitro* and *in vivo*, with inhibitors of Hsp90, calcineurin and TOR the most prominent among them[15-18]. Combination therapy using antifungals together with such inhibitors has been proposed as a promising strategy to extend the efficacy of current drugs[19-24,25,26,27]. In addition, several psychotherapeutic agents such as fluoxetine, fluphenazine or sertraline can enhance FLC activity against fungal species[21,28-30]. Whether such adjuvants affect therapeutic outcomes remains to be addressed.

Persistent candidemia, defined as the failure to clear a bloodstream infection caused by a susceptible organism[12,31,32], is associated with increased mortality. In one study, the mortality

rate was 54% among infections with persistent candidemia and only 3% among those with non-persistent candidemia[33]. Mechanisms underlying persistent candidemia may include variability in the pharmacology of the drug, suboptimal dosing, presence of fungal biofilms on indwelling catheters, and reduced immunity. We posit that some responses to the drug are not captured by measuring the MIC alone and that additional parameters could be used to predict the likelihood that a clinical isolate might respond poorly to antifungal drugs. Furthermore, understanding the mechanisms that underlie these parameters is critical for the development of new therapeutic approaches against persistent *Candida* infections.

MIC measurements have been optimized to minimize or ignore residual fungal growth[9,34,35], termed 'tolerance' or 'trailing growth', which has been discussed in the literature for over 20 years[36,37] and is detected in 25-60% of clinical isolates[4,10,19,38-44]. This recommendation is based upon studies of acute infections using the mouse model of bloodstream candidiasis[45-47], and the observation that isolates with high trailing growth in mucosal infections respond positively to short term antifungal treatment, despite later recurrence of infection[48]. Trailing growth is sensitive to environmental conditions, including pH, temperature and nutrients[3,49,50] and is usually detected in liquid cultures. Definitions of 'tolerance' vary and generally describe survival or growth above inhibitory concentrations[2,10,28,38,51-56], detected as slow growth within the zone of inhibition using E-strips or disk diffusion assays [57,58], or in broth microdilution assays[38,39]. Tolerance can be affected by several adjuvant drugs[19-24], iron levels[19,59], genes involved in vacuolar protein sorting[38,47], as well as calcium flux[28,55,59-61]. However, the precise relationship between the outcome of fungal infections and tolerance or trailing growth has not been determined. Because tolerant cells continue to divide in the presence of antifungals, we postulated that they contribute to the persistence and/or recurrence of fungal infections.

Here, we measured susceptibility and tolerance in a broad range of clinical isolates spanning the major *C. albicans* clades[62-64] and asked how these parameters influence fungal infection outcomes. We analyzed disk diffusion assays using *diskImageR*, and quantified the

radius (RAD) of the zone of inhibition, a parameter that relates to the MIC[65], and the fraction of growth (FoG) within the zone of inhibition, a parameter that measures tolerance[19,38,50,66-68]. We found that a range of adjuvant drugs, used in combination with FLC, increased drug cidality by reducing FoG and not MIC and were effective both *in vitro* and *in vivo* at inhibiting strains with high (and not low) FoG levels. Finally, highly tolerant isolates were associated with persistent candidemia, suggesting that knowing the tolerance level of an infecting isolate may have important clinical implications and may inform treatment options.

Results

Tolerance measured as FoG is distinct from drug resistance. We quantified drug responses in *C. albicans* isolates from different genetic backgrounds and types of infections using *diskImageR,* a quantitative analysis tool that measures RAD, the radius of the zone of inhibition, an indicator of susceptibility that relates to MIC[69,70], and FoG, the fraction of growth within the zone of inhibition, relative to the maximum possible growth[65] (Fig. 1a). A screen of 219 clinical isolates (Supplementary Table 1) revealed that FoG levels ranged widely from 0.10 to 0.85 and did not correlate with RAD levels (Fig. 1b,c), indicating that FoG and RAD measure independent drug responses. FoG was detected in response to other drugs including fungistatic antifungals (azoles, 5-fluorocytosine) and, to a lesser degree, to fungicidal agents (echinocandins, polyenes) (Supplementary Fig. 1a). Antifungal responses varied widely in different *Candida* species as well as in *S. cerevisiae* (Supplementary Fig. 1b). For example, *C. glabrata* exhibited the highest tolerance to azoles, followed by *C. tropicalis* and *C. krusei,* while *S. cerevisiae* had low tolerance to azoles and intermediate tolerance to echinocandins and polyenes.

Broth microdilution assays define the MIC_{50} - the lowest drug concentration that inhibits 50% of growth at 24 h (termed MIC throughout the manuscript). Most reports of 'trailing growth' or 'tolerance' monitor growth at 48 h[48-50,71]. We quantified supra-MIC growth (SMG) at 48 h

(average growth per well above the MIC_{50}, normalized to growth without FLC; Fig. 1d). Most isolates exhibited some level of SMG at 48 h, while MIC levels remained unchanged between 24 and 48 h (Fig. 1e-g). Thus, SMG provides a parameter that, like FoG, is distinct from MIC.

Importantly, cells exhibiting FoG in disk assays or SMG in broth assays, are not due to the emergence of drug resistance. Thus, for a given isolate, FoG and SMG levels were reproducible for cells taken from inside or outside the zone of inhibition, or for cells taken from wells above or below the MIC (Supplementary Fig. 2a, b). These cells yield progeny indistinguishable from other cells in the population, and thus are the result of phenotypic heterogeneity rather than genetic alteration. Consequently, tolerance is due to growth heterogeneity in the population and is stable for a given isolate.

While SMG and FoG correlated well with each other ($R^2 = 0.82$, $P < 0.01$), there was no relationship between FoG and RAD ($R^2 < 0.01$), or SMG and MIC ($R^2 = 0.25$, $P < 0.01$, Supplementary Fig. 2c). FoG and SMG therefore reflect similar features of growth at supra-MIC concentrations that are distinct from drug susceptibility/resistance, as measured by RAD or MIC, which are concentration-dependent parameters. Accordingly, whereas RAD increased with increasing drug concentrations in the disk (Fig. 1h), FoG remained similar irrespective of drug concentration. Similarly, SMG levels remained constant across a broad range of supra-MIC concentrations (Fig. 1e). Thus, tolerance measured as FoG or SMG is not dependent upon drug concentration, highlighting the distinctive nature of tolerance relative to susceptibility/resistance.

Environmental modulation of drug responses. FoG and SMG levels were reduced at pH 4.5 relative to pH 7, while RAD/MIC levels remained relatively stable (Supplementary Fig. 3a,b). FoG/SMG values also decreased with higher temperatures (37-41°C) while RAD/MIC levels showed less variation with increasing temperature (Supplementary Fig. 3c,d). For some strains, including SC5314, RAD and/or FoG levels varied considerably depending on the growth media

(Supplementary Fig. 3e). A series of strains derived from SC5314 by passaging were particularly sensitive to media differences, with lower RAD and higher FoG levels on rich medium (YPD) than on casitone medium (Supplementary Fig. 3f), emphasizing that assays must be performed under consistent conditions to ensure reproducible results. Importantly, differences in genetic background can have a major effect on how *C. albicans* strains respond to environmental conditions.

Subpopulation growth dynamics. To ask if tolerance reflects the size of a dividing subpopulation at supra-MIC concentrations, we compared the number of cells that form colonies (CFUs) in the presence of supra-MIC FLC concentrations to total CFUs without drug. CFUs on drug ranged between 2% and 98% of the total population and correlated with FoG levels (Fig. 2a, $R^2 = 0.91$, $P < 0.01$). The proportion of the subpopulation that grew at supra-MIC FLC in liquid cultures did not change with inoculum size (Supplementary Fig. 3g), indicating that FoG/SMG is independent of cell density. Importantly, these results establish that FoG levels represent the proportion of the population that can form colonies or grow above the MIC.

Growth dynamics were also monitored using microcolony assays, in which time-lapse microscopy follows colony area/size (Fig. 2b)[72]. As expected[73], exponentially growing cells plated on 10 µg/ml FLC did not stop growing immediately. Rather, most cells continued dividing for ~5 h, and then slowed or stopped dividing to different degrees (Fig. 2c,d and Supplementary videos 1-4). In high FoG isolates (e.g., SC5314), a large proportion of the cells yielded microcolonies, while in low FoG isolates (e.g., P87), more cells stopped dividing (black dots in Fig. 2b). Differences in growth rates became apparent after 10-15 h in FLC (Fig. 2d), supporting the idea that different subpopulations have different growth dynamics, and that high FoG strains produce a larger subpopulation of growing colonies than low FoG isolates.

The dynamics of colony growth on agar plates was also examined using *ScanLag,* a flatbed scanner/image analysis pipeline[74] that we adapted for use with *C. albicans*. Here, the

area occupied by light pixels and the change in this area over time are proxies for colony size and growth rate, respectively[74]. Different *C. albicans* isolates exhibited different initial time of colony appearance (ToA) on medium without drug (Supplementary Fig. 4). At 10 μg/ml FLC, the ToA was delayed relative to the drug-free condition (except for resistant strains such as T101, Fig. 2e,f). Notably, the ΔToA (ToA on FLC – ToA without FLC) of high FoG isolates was shorter than that of low FoG isolates (Fig. 2f), and correlated with overall FoG levels (Fig. 2g). This suggests that high FoG strains overcome the inhibitory pressures of the antifungal more efficiently than low FoG strains. Consistent with this, in liquid assays with drug, highly tolerant isolates also displayed shorter lag times than related isolates with low tolerance levels (Supplementary Fig. 5a).

A number of *C. albicans* growth parameters did not correlate with FoG levels. These included cell viability in the presence of drug (Fig. 2h), consistent with FLC being fungistatic rather than fungicidal. Unlike tolerant bacteria, which display reduced growth rates and longer colony appearance times[2,75-77], antifungal tolerance did not correlate with slower growth in three sets of related *C. albicans* strains grown in liquid without drug, including: (1) passaged derivatives of SC5314 with altered FoG levels, (2) a slow-growing clinical isolate (P37005) and faster growing derivatives[78] and (3) a *clb4* mutant[79] with delayed cell cycle progression relative to control strains (Supplementary Fig. 5b). Furthermore, exponential and stationary phases yielded similar FoG levels (Supplementary Fig. 5c), unlike phenotypic drug resistance in bacteria[80]. Growth parameters (colony size and growth rate, liquid growth rate and lag phase duration) also failed to show any correlation with FoG levels (Supplementary Fig 5d,e). This implies that tolerance is not simply a reflection of faster growth in the presence or absence of drug. Rather, it reflects two aspects of *C. albicans* growth dynamics: a larger subpopulation able to form colonies at supra-MIC drug concentrations (Fig. 2a), and a faster relative recovery in response to fungistatic pressures.

Decreased intracellular drug levels underlie increased tolerance. A recently developed fluorescent azole probe, FLC-Cy5[81], provides a powerful tool to monitor intracellular drug levels and uptake rates using flow cytometry (Fig. 3a). The initial rate of FLC-Cy5 uptake per cell varied between strains and showed a weak inverse correlation with FoG levels (R^2 = 0.64, P = 0.12, Fig. 3b). By contrast, steady state FLC-Cy5 levels at 24 h correlated inversely with FoG levels (R^2 = 0.8, P < 0.01, Fig. 3c). Cells were categorized as having low, mid, and high levels of FLC-Cy5 (at 24 h). FoG levels inversely correlated with the proportion of cells that contained high FLC-Cy5 levels (R^2 = 0.82, P = 0.04) and positively correlated with the proportion of cells containing mid FLC-Cy5 levels (R^2=0.81, P = 0.05, Fig. 3d,e).

Based on the assumption that the steady state drug levels are influenced by both drug efflux and uptake, we measured efflux of rhodamine-6-G (R6G), a dye removed primarily via the ABC class of transporters[82]. In general, the rate of R6G efflux was higher in the presence, than in the absence, of FLC, with SC5314 as the notable exception (Fig. 3f and Supplementary Fig. 6a). Yet, efflux rates did not correlate with FoG under any of the conditions tested (Supplementary Fig. 6b, R^2 < 0.2). Thus, the determinants of steady state intracellular FLC levels are complex, and include uptake and efflux rates as well as other factors (Fig. 3g).

Adjuvant drug combinations clear tolerance and do not alter resistance. Combination therapies has the potential to extend the lifespan of the few available antifungal drug classes[24,83-85]. We tested a series of adjuvant drugs to determine their quantitative effect on fungal responses when used together with FLC. Most adjuvants significantly reduced FoG, including geldanamycin and radicicol, which inhibit Hsp90 activity[15,27,61,86], cyclosporine A and FK506, which inhibit calcineurin[87-89] and staurosporine, which inhibits PKC1 activity[90]. In addition, other adjuvants not directly connected to Hsp90 function also reduced FoG, including aureobasidin A, which inhibits sphingolipid biosynthesis[20]; rapamycin, an inhibitor of the mTOR signaling pathway[22,91]; tunicamycin, an inducer of the unfolded protein response pathway[92-94];

fluoxetine, a serotonin inhibitor[21]; and fluphenazine, an antipsychotic drug that stimulates ABC transporter expression and indirectly inhibits calcineurin via calmodulin[23,28,95]. FLC + adjuvant cleared tolerance for all 7 clinical isolates tested (Fig. 4a,b), as well as for a longitudinal series from a single HIV patient[96,97] that had acquired resistance over time, and for a set of persistent and non-persistent clinical isolates (Supplementary Fig. 7a-d). Importantly, most adjuvants had little or no effect on RAD/MIC levels (Fig. 4a,b and Supplementary Fig. 7a-d), and thus are not expected to affect resistance in standard susceptibility assays[34,98].

Hsp90-dependent responses affected tolerance and not susceptibility/resistance measured as MIC (at 24 h). Consistent with this, the effects of temperature and Hsp90 inhibitors correlated well with FoG (R^2 = 0.93, Supplementary Fig. 7e) and only partially with RAD (R^2 = -0.61, Supplementary Fig. 7f). Thus, temperature inhibition of Hsp90 affects tolerance and not resistance *per se*. Furthermore, FoG levels were not affected by Hsp90 steady state protein levels, as the amount of Hsp90 did not correlate with FoG (R^2 = 0.07, Supplementary Fig. 7g). Because inhibitors of calcineurin and Hsp90 are known to affect FLC cidality[15,24,27,61,67,88,99,100], we asked whether other adjuvant drugs have a similar effect. All tested combinations were cidal (Fig. 4c and Supplementary Fig. 7h), indicating they have a profound effect on cell viability at supra-MIC FLC concentrations and implying that stress pathways make essential contributions to tolerance.

Consistent with the adjuvant drug responses, genes involved in several pathways, including calcineurin-[101] and PKC signaling[90], primarily affect FoG and not RAD (Fig. 4d, Supplementary Fig. 8, Supplementary Tables 3, 4, and Supplementary Text). In addition, *IRO1*, which is involved in iron homeostasis[19] and *VPS21,* which is involved in vacuolar trafficking[38], affected FoG and not RAD. Thus, many genetic pathways affect the ability of subpopulations of cells to grow in the presence of supraMIC FLC concentrations, including Hsp90-dependent and -independent responses that are due to tolerance rather than resistance.

Adjuvant drugs improve FLC efficacy against high FoG strains *in vivo*. Given that the beneficial effects of adjuvant drugs are more evident on high FoG strains, we asked if adjuvant therapy would distinguish between levels of tolerance in an infection model. *Galleria mellonella* larvae were used to test potential *in vivo* differences between isolates with different tolerance levels, both with respect to their ability to cause disease, and with their ability to respond to therapy with FLC alone or FLC plus the adjuvant fluphenazine[29,102] (FNZ, Fig. 4a). A series of isolates was derived by passaging the SC5314 strain in the presence or absence of FLC. The resulting isolates had indistinguishable RAD but distinct FoG levels relative to the parental strain (Supplementary Fig. 9a and Supplementary Table 1).

G. mellonella larvae infected with fungal cells were treated with either PBS (control), FLC, or combination therapy (FLC and FNZ) (Fig. 5a). SC5314 and derived strains with similar FoG levels killed all larvae within 9-14 days. Importantly, these lower FoG isolates had similar responses to FLC and to the FLC+FNZ combination: they rescued up to 17% of the infected larvae (Fig. 5b,c and Supplementary Fig. 9b). By contrast, high FoG strains displayed delayed killing and decreased virulence in the larvae, and did not respond to FLC alone (Fig. 5d and Supplementary Fig. 9b). Notably, the FLC+FNZ combination significantly improved the outcomes for high FoG strains relative to FLC alone and PBS-control groups: larval death was delayed and up to 50% of larvae infected with high FoG strains survived the experiment (Fig. 5d and Supplementary Fig. 9b). Similar results were obtained with a low FoG clinical isolate (readily cleared by FLC therapy) when compared with a high FoG isolate (that persisted in the bloodstream during multiple rounds of FLC therapy) (Supplementary Fig. 9c). Presumably, FLC+FNZ significantly decreased larval killing by rendering FLC cidal for those cells growing at supra-MIC concentrations. Thus, *in vivo* responses to azoles and to combination therapies differed for different isolates according to their tolerance levels.

Persistent candidemia is associated with highly tolerant isolates. Echinocandins are considered the optimal line of therapy for patients with candidemia, yet FLC remains a frontline drug for systemic *C. albicans* infections[103], especially in low income countries[104]. Treatment with FLC often fails despite isolates being drug-susceptible when tested *in vitro,* and rates of persistent candidemia are often higher in patients treated with FLC rather than with echinocandins[105,106]. To examine possible connections between susceptibility and tolerance levels, we collected sets of clinical isolates from patients with candidemia that were either efficiently cleared by a single course of FLC treatment (non-persistent) or that persisted in the host despite extended FLC therapy (Fig. 6a, Supplementary Fig. 10a, see detailed isolate description in Methods).

The drug responses of persistent and non-persistent isolates and several control strains displayed similar RAD and MIC levels (0.25-1 μg/ml), well below those of resistant strains (clinical MIC breakpoint = 4 μg/ml), when assayed at both 24 and 48 h (Fig. 6b and Supplementary Fig. 10b,c). Strikingly, FoG/SMG levels differed significantly between the two groups of clinical isolates, especially when compared at 48 h (Fig. 6b,c) and, as expected, correlated well with one another (Supplementary Fig. 10d, $R^2 = 0.62$). Importantly, persistent candidemia isolates displayed higher FoG/SMG levels than those readily cleared upon FLC treatment. In fact, many persistent isolates had FoG levels higher than 0.5, indicating that over half of the cells in the population could grow, albeit slowly, in the presence of FLC (Fig. 6b). Taken together, these experiments demonstrate that tolerance is an intrinsic property distinct from drug susceptibility, and that tolerance levels correlate with infections that resist azole treatment in the clinic.

Discussion

Currently, decisions about therapeutic strategies to treat *Candida* infections are based upon patient status, infecting species and antifungal susceptibility, with clinical MIC assays

designed to avoid the detection of tolerance[3,34]. Here, quantification and characterization of tolerance across *C. albicans* isolates found that many of them exhibit tolerance, defined as the ability of a subpopulation of cells to grow slowly at supra-MIC concentrations. Tolerance is related to phenomena previously described as 'trailing growth' [3,38,39,49,50,67,71,107], 'tolerance'[10,19,40-42] or Hsp90-dependent 'resistance'[15,51,61,90,108]. Studying growth dynamics and quantifying tolerance revealed that it is: 1) a subpopulation effect and the size of the subpopulation is stable; 2) due to slow growth in drug stress; 3) correlates with intracellular drug levels; 4) dependent upon stress response pathways, and 5) mechanistically distinct from resistance. Several adjuvants completely cleared FoG without altering susceptibility (MIC) and, when combined with the fungistatic drug FLC, yielded a fungicidal cocktail. Consistent with this, combination therapy was most effective *in vivo* at treating infections by high tolerance strains, whereas the adjuvant did not improve FLC efficacy against low FoG isolates. Furthermore, *C. albicans* isolates that cause persistent candidemia exhibited significantly higher tolerance than isolates readily cleared by FLC. Thus, quantitatively measuring tolerance levels of infecting isolates may provide important prognostic insights concerning both the success of FLC therapy as well as the potential efficacy of combination therapies.

The subpopulation effect of tolerance is readily detected on agar plate assays, where individual cells and their clonal progeny are evident; in liquid assays, cells become mixed and subpopulation effects are more difficult to distinguish. Growth dynamics in colonies[74], microcolony formation[73] and liquid growth assays all suggest tolerance correlates with the degree of growth after drug exposure. This implies that a subpopulation of cells is inherently more able to adapt to drug than the rest of the population. Since the size of such subpopulations appears stable, we suggest that tolerance is a function of cell physiology and environmental responsiveness that differs between genetic backgrounds and growth conditions.

We discovered that isolates with higher tolerance levels have more cells with lower intracellular drug levels, but tolerance is not a function of either uptake or efflux rates, despite

the well-known role of efflux in drug resistance[109-118]. The factors other than uptake and efflux that impact intracellular FLC levels remain to be determined.

Adjuvant drugs increase FLC cidality and efficacy via tolerance, not resistance. A novel insight from this work is that inhibitors of cellular stress improve fluconazole efficacy, primarily via their effect on tolerance and not resistance. This has two important implications. First, the subpopulation nature of tolerance suggests that these stress pathways must exhibit cell-to-cell variation. Second, the contributions of stress response pathways differ considerably between isolates, albeit in a manner that maintains population heterogeneity (and the size of the tolerant subpopulation) as a heritable feature of the given strain.

Tolerance is clearly related to the Hsp90-dependent response and distinct from *bona fide* resistance. Hsp90 and calcineurin are well known to affect fungal drug responses, including the cidality of azoles[19,67,87,89,119-122]. How the TOR pathway, the unfolded protein response, PKC signaling, sphingolipid synthesis, iron homeostasis, as well as fluoxetine and fluphenazine affect drug responses and increase FLC cidality remains to be determined.

The distinction between resistance and tolerance is consistent with the mechanisms that impact them: resistance mechanisms directly affect the drug target or its concentration in the cell, thereby enabling efficient growth in the presence of the drug[14,111]. By contrast, tolerance reflects stress response strategies that are indirect and may enable survival despite the continued ability of the drug to interact with its target, to remain in the cell and to affect cell growth. Stress responses can modulate physiology, for example membrane[59,123,124] or cell wall integrity[125] and the aggregation of proteins into stress granules or other physiological switches[126], thereby minimizing deleterious cellular responses to the drug.

Differences between antifungal and antibacterial tolerance. The growth properties of cells at supra-MIC concentrations measured here with FLC, a fungistatic drug, contrast with those

361 measured for antibacterial tolerance in bactericidal drugs. This likely reflects distinct modes of
362 action between static and cidal drugs as well as different molecular mechanisms of stress
363 responses in eukaryotes and bacteria. Antibacterial tolerance generally involves a longer lag
364 phase for the majority of the population[75-77]. By contrast, antifungal tolerance involves the earlier
365 appearance of a subpopulation of cells that continue to grow in the presence of drug and, unlike
366 'phenotypic resistance' described for bacteria[127], is not dependent upon growth phase or cell
367 density.
368
369 **Clinical implications**. This study revisited the question of whether supra-MIC growth is
370 clinically relevant and, by inference, whether the stress pathways that mediate it represent
371 important drug targets. Previous work suggested that trailing growth was not important for
372 virulence in either mouse models[45,46] or infection outcomes in the human host[48]. However, these
373 studies analyzed short-term responses, rather than persistence or recurrence of *Candida*
374 infection over longer time frames. Here, both *in vivo* and clinical studies provide a proof of
375 principle suggesting that retrospective and prospective clinical studies that measure tolerance
376 are warranted. We posit that monitoring FoG/SMG in standard clinical assays may have
377 prognostic value for the likelihood of a persistent infection, for the responsiveness of a given
378 isolate to FLC, as well as for the synergism of an adjuvant drug with FLC. Furthermore, in
379 developing countries where azoles remain the major antifungals in use, measuring tolerance
380 may be especially relevant and the addition of low cost adjuvant drugs could significantly impact
381 treatment outcomes (e.g.,[128]). Understanding the contribution of tolerance to the progression of
382 fungal infections not only can provide fundamental insights into the biology of fungal
383 subpopulation behaviors, but also has the potential to inform clinical practices.
384
385 **Methods**

386 ***C. albicans* isolates.** All strains (Supplementary Table 1) were streaked onto rich media (YPD)
387 plates and grown for 24 h at 30°C. A single colony from each strain was arbitrarily selected and
388 frozen in 15% glycerol and stored at -80°C for all assays. For each mutant tested, we used
389 genetically matched parental control strains and, where appropriate, nutrient supplements were
390 used to compensate for auxotrophies (Supplementary Table 4).
391 Isogenic SC5314 low and high FoG isolates were obtained by sequentially passaging
392 SC5314 every 24 h in YPD (1/100 dilutions, ~84 generations) either with or without 1 μg/ml
393 FLC. Persistent and non-persistent clinical isolates were obtained from patients with
394 candidemia that were investigated by Dr Colombo during several candidemia surveys[129].
395 Fungal isolates were obtained from two groups of patients: patients with a single episode of
396 candidemia, for which infection was resolved after the first course of antifungal therapy, and
397 patients with persistent candidemia. Persistent candidemia was defined here as two or more
398 blood cultures positive for *C. albicans*, on one or more days apart, despite at least 3 days of
399 antifungal therapy with FLC. Non-persistent isolates (NP1-7) were cleared from the
400 bloodstream soon after FLC treatment was initiated and treatment was continued for an average
401 of 16 days. In contrast, persistent infections in 12 patients yielded serial isolates both prior to
402 and throughout the course of treatment, with 3 to 9 isolates per patient treated for an average of
403 20 days (P, S01-S12, Supplementary Fig. 10a). Persistent candidemia in these patients
404 occurred despite clinical MIC assays having established that all isolates were FLC susceptible,
405 with MIC levels < 1 μg/ml. While each patient had distinct clinical backgrounds and trajectories,
406 the two groups were matched in terms of age, underlying conditions, time of central venous
407 catheter removal, and first line of antifungal therapy. Patients received intravenous FLC as first
408 line of therapy and the initial time of therapy did not differ between persistent and non-persistent
409 infections. In some cases of persistent candidemia, antifungal therapy was continued with either
410 caspofungin or amphotericin B (Supplementary Fig. 10a). Of the 19 patients, 7 patients died
411 during the 30 day follow up, 6 of which were unable to clear the fungal infection, although

412 causality between infection and death could not be determined. Isolates from patients with
413 cancer, neutropenia, endocarditis, deep-seated *Candida* infections, corticosteroid or other
414 immunosuppressive drug exposure were excluded from the study. All ethical regulations were
415 observed and the study was approved by the Ethical Committee of the Federal University of
416 São Paulo (January, 2016, NO 9348151215).
417
418 **Strain construction.** To disrupt the two alleles of the *RCN2* gene, we amplified (using primers
419 BP1440 and BP1441, Supplementary Table 5) the flanking sequence of ORF C7_01700W
420 using BJB-T 2 (*HIS1*) and BJB-T 61 (*ARG4*) plasmids as a template (Supplementary Table 5).
421 Strain YJB-T65 was transformed with this PCR product to generate heterozygote mutant YJB-T
422 2214 (*rcn2*::*HIS1*) and subsequently homozygote mutant YJB-T2227 (*rcn2::HIS1/rcn2*::*ARG4*).
423 The disruptions were verified using primers BP1444 and BP1445.
424
425 **Broth micro dilution assays.** Minimal inhibitory concentration (MIC) for each strain was
426 measured using CLSI M27-A2 guidelines[98] with minor modifications as follows. Strains were
427 streaked from glycerol stock onto YPD agar and grown for 24 h at 30°C. Colonies were
428 suspended in 1 ml PBS and diluted to 10^3 cells/ml in a 96-well plate with casitone containing a
429 gradient of two-fold dilutions per step of FLC, with the first well contain no drug. For persistent
430 and non-persistent clinical isolates, cells were grown overnight in YPD at 30°C and diluted to
431 10^4 cells/ml in YPD containing a gradient of two-fold dilutions per step of FLC. MIC_{50} levels
432 were determined after 24 h or 48 h by taking an optical density reading (OD_{600}) by a Tecan
433 plate reader (Infinite F200 PRO, Tecan, Switzerland). MIC_{50} levels (shown as yellow lines on
434 broth microdilution assays heatmaps) were determined as the point at which the OD_{600} had
435 been reduced by ≥50% compared to the no-drug wells.
436

Disk diffusion assays. The CLSI M44-A2 guidelines for antifungal disk diffusion susceptibility testing[130] were followed with slight modifications. In brief, strains were streaked from glycerol stocks onto YPD agar and incubated for 24 h at 30°C. Colonies were suspended in 1 ml PBS and diluted to 1 x 10^6 cells/ml. 2 x 10^5 cells were spread onto 15 ml casitone plates (9 g/l Bacto casitone, 5 g/l yeast extract, 15 g/l Bacto agar, 11.5 g/l sodium citrate dehydrate and 2% glucose, 0.04 g/l Adenine, 0.08 g/l Uridine). For persistent and non-persistent clinical isolates, cells were grown overnight in YPD and 10^5 cells were spread onto 15 ml YPD plates. To facilitate comparisons between casitone and YPD disk diffusion assays, a subset of control strains with different FoG levels were included in both types of assays (SC5314, GC75, P87). The fraction of growth and radius of inhibition levels, referred to as FoG and RAD throughout the manuscript, represent parameters measured at 20% drug inhibition (FoG_{20} and RAD_{20}, respectively). For disk diffusion assays performed with auxotrophic strains, supplementary amino acids were added to the media (0.04 g/l Histidine and 0.04 g/l Arginine). For disk assays with drug adjuvants, the following concentrations of drugs were used: 0.5 µg/ml geldanamycin, 0.5 µg/ml radicicol, 0.5 µg/ml FK506, 0.4 µg/ml cyclosporine A, 20 µg/ml fluoxetine, 5 ng/ml aureobasidin A, 0.5 ng/ml rapamycin, 10 µg/ml fluphenazine, 50 µg/ml doxycycline, 12.5 ng/ml staurosporine and 0.25 µg/ml Tunicamycin. A single 25 µg FLC disk (6 mm, Oxoid, UK or Liofilchem, Italy) was placed in the center of each plate, plates were then incubated at 30°C for 48 h, and each plate was photographed individually. Analysis of the disk diffusion assay was done using the *diskImageR* pipeline[65] and the R script is available at https://github.com/acgerstein/diskImageR/blob/master/inst/walkthrough.R . Several controls indicated that drug in the disk is stable: incubation of the disk on the plate for 24 h prior to plating cells did not change FoG levels. In addition, incubation of the disk on the plate for 24 h prior to plating cells did not affect FoG levels, neither did addition of a fresh disk to the plate after 24 h.

ScanLag assay. The ScanLag assay was adapted from[74] with minor modifications. Strains were streaked from glycerol stocks onto YPD agar and incubated for 24 h at 30°C. Colonies were suspended in 1 ml PBS, diluted to 10^4 cell/ml and ~ 500 were spread onto casitone plates with or without 10 µg/ml FLC (Sigma-Aldrich, St. Louis, MO). Plates were placed on the scanners at 30°C and scanned every 30 min for 96 h. Image analysis was done in MATLAB using the "ScanLag" script[74] that was adapted for yeast cells by changing the identification of the size of the colony to a minimum of 20 pixels.

Viability assays. Replica plating was performed from disk diffusion plates that were incubated at 30°C for 48 h. Master plates were inverted and pressed firmly on a sterile cotton velveteen stamp and then transferred to new casitone plates containing no drug. Replica plates were incubated at 30°C for 48 h, and then each plate was photographed individually.

Enzyme-linked immunosorbent assay (ELISA). The ELISA protocol was modified from[131]. Briefly, *C. albicans* cells were grown for 6 h at 30°C with shaking (220 RPM) in YPD with or without 10 µg/ml FLC (Sigma-Aldrich, St. Louis, MO) and harvested at exponential phase (OD_{600} 0.6–0.8). Cells were centrifuged for 10 min (3000 rpm, 4°C), and washed once with ice-cold PBS. Pellets were resuspended in 200 µl lysis buffer (50 mM Hepes pH 7.5, 150 mM NaCl, 5 mM EDTA, 1% Triton X100, protease inhibitor cocktail (Roche Diagnostics)) together with acid-washed glass beads. Cells were then mechanically disrupted by vortexing for 30 min at 4°C. Cell lysates were diluted 1:10 in PBS and subjected to BCA analysis (Pierce Biotechnology, Rockford, IL) to determine protein concentrations. Cell lysates at 10 µg/ml concentration were incubated in 96-well ELISA plates for 18 h at 4°C. Wells were washed with PBST (PBS +0.05% Tween-20), blocked with 1% skim milk in PBST for 2 h at 37°C and washed. Rabbit polyclonal anti Hsp90 antibody (Dundee Cell Products, Scotland) was diluted

1:1000 in blocking buffer applied overnight at 4°C. Horseradish peroxidase-coupled donkey anti-rabbit IgG (1:1000 dilution, Jackson ImmunoResearch Laboratories, West Grove, PA) was incubated for 1 h at 37°C followed by washing. Detection was done with TMB (3,3',5,5'-tetramethybenzidine). The reaction was terminated with 0.16 M sulfuric acid and absorbance was measured at 450 nm in an ELISA plate reader.

FLC-Cy5 uptake measured by flow cytometry. *C. albicans* cells were grown overnight in YPD media at 30°C**.** Cultures where diluted 1:100 in 3 ml casitone medium and incubated for 3 h at 30°. Drugs were added to a final concentration of 10 µg/ml for FLC, and 1 µg/ml for FLC-Cy5[81]. Cells were harvested every 30 min and diluted 1:4 in 50% TE (50 mM Tris pH 8:50 mM EDTA). Data was collected from 25,000-35,000 cells per time point using 561 nM EX and 661/20 nM EM in a MACSQuant flow cytometer and gated to by SSC<10^3 A.U and FSC>10^4 A.U in (SSC vs FSC) to eliminate small debris particles. Analysis was done using FlowJo 8.7 software.

Efflux of Rhodamine 6G (R6G) as measurement of drug efflux capacity. The assay was adapted from[132] with minor modifications. In brief, strains were stre
aked from glycerol stock onto YPD plates and incubated for 24 h at 30°C. Colonies were resuspended in 3 ml casitone medium and grown overnight in 30°C. Cultures where diluted 1:100 in 5 ml casitone medium and incubated for 3 h at 30°. Cells were centrifuged, washed in 5 ml PBS (pH 7), and resuspended in 2 ml PBS with or without 10 µg/ml FLC. Cells suspensions were incubated for 1 h at 30°C and R6G (Sigma-Aldrich, St. Louis, MO USA) was added at 10 µg/ml to allow R6G accumulation (1 h). Next, cells were washed twice with PBS at 4°C, and resuspended in a final volume of 300 µl PBS. 50 µl of individual suspensions were diluted in 150 µl PBS and aliquoted into a 96-well microtiter plate. Baseline emission of

fluorescence (excitation 344 nm, emission 555 nm) was recorded for 5 min in a Tecan plate reader at 30°C (Infinite F200 PRO, Tecan, Switzerland), in relative fluorescence units (RFU), and 1% D-glucose was next added to each strain to initiate R6G efflux. Negative controls contained no glucose and data points were recorded for 90 min in triplicates at 1 min intervals.

G. mellonella virulence assays. *G. mellonella* larvae were obtained from Vanderhorst Wholesale (Saint Marys, OH) and the infection protocol was adapted from Li *et al*[133]. Larvae were kept at 15°C and used within 1 week of delivery. Larvae were randomly selected for each experiment in groups of 12 and those showing signs of melanization were excluded. *C. albicans* inoculums were prepared from cultures grown overnight at 30°C in YPD and washed twice with sterile PBS. Cells were counted using a hemocytometer and adjusted to 3 x 10^7 cells/ml in sterile PBS. Each larva was initially injected with 3 x 10^5 cells via the last left pro-leg using a 10 µl glass syringe and a 26S gauge needle (Hamilton, 80300). A second injection with either FLC (1 mg/kg), FLC + fluphenazine (FNZ, 10 mg/kg), or sterile PBS was done via the last right pro-leg 1.5-2 h post infection. The inoculum size was confirmed by plating of fungal cells on YPD. Infected larvae and PBS injected controls were maintained at 37°C for 14 days and checked daily. Larvae were recorded as dead if no movement was observed upon contact. Virulence assays were performed with strain SC5314, with SC5314-derived isolates passaged for 12 days in either YPD alone (2 'low' FoG isolates) or YPD plus 1 µg/ml FLC (4 'high' FoG isolates), and with isolates NP03 and S12-01 from a clinical isolate set (see Supplementary Table 1). Experiments were performed in duplicate (n = 24 larvae) and statistical differences between larval groups were tested using the Mantel-Cox test. Negative controls included PBS, FLC alone or FLC + FNZ for groups of 24 larvae. No significant killing of larvae was observed in either of these conditions.

538 **Growth assays.** To determine growth parameters (doubling time and lag phase duration), *C.*
539 *albicans* cells were seeded at a concentration of 2 x 10^5 cells/ml into 96-well plates containing
540 YPD media. Plates were incubated for 48 h at 30°C with continuous shaking in a Tecan plate
541 reader (BioTek) and the optical density reading (OD_{600}) was recorded every 15 min.
542 Measurements of doubling time and lag phase duration were determined using BioTek Gen5
543 software and from 3 biological replicates, each performed in duplicate.
544
545 **Microcolony assays.** Microcolony assays were adapted from[72] with minor modifications.
546 Colonies were resuspended in 3 ml casitone medium and grown overnight in 30°C. Cultures
547 were diluted 1:30 in casitone medium and incubated at 30°C until cultures reached logarithmic
548 phase (~3-4 h) and diluted to 10^4 cells/ml in casitone medium. For microscopy, glass-bottomed
549 24-well plates (De-GROOT, Israel) were coated with 1 ml of a 200 µg/ml Concanvalin A solution
550 (Type VI, Sigma-Aldrich, St. Louis, MO USA) for 3-4 h. Wells were washed twice with 1 ml
551 ddH20 and 10^4 cells/ml in a 2 ml volume were added to wells with or without 10 µg/ml FLC.
552 Plates were sealed with an optically clear film (Axygen, Corning, Israel) and spun at
553 1200 rpm for 1 min. Images where captured in 100 fields per well for 48 h in 1 h intervals using
554 a Nikon Ti Eclipse microscope equipped with a full-stage environmental chamber (set to 30°C)
555 with a Nikon Plan Apo 10x (0.45 numerical aperture) objective using Nikon Elements AR
556 software. The focusing routine utilized manual assignment for each well based on a single
557 field[134]. Custom software for conducting microcolony experiments, including computing and
558 tracking microcolony areas over time was adapted from[72]. Specific growth rates were calculated
559 for 1500-5000 colonies per strain[72] by regressing the natural log of microcolony area over time.
560 Growth rates were calculated separately for two time intervals (0-5 h and 10-15 h) and required
561 to have an R^2>0.9. Replicate wells (3 per condition) were consistent and growth rate
562 distributions were pooled.
563

564 **Statistical analyses.** All experiments represent the average of two or more biological
565 replicates, with two technical replicates of each. Error bars represent the standard deviation.
566 Statistical analyses were performed using two-tailed Student's t tests, one way ANOVAs and
567 Tukey's multiple comparison tests using Microsoft Excel 2016 (Microsoft) and Prism 6
568 (GraphPad); R^2 tests were used for linear regressions. Significance was assigned for *P* values
569 smaller than 0.05, asterisks denote *P* values as follows: ***, $P < 0.001$; **, $P < 0.01$; *, $P < 0.05$.
570
571 **Data availability.** The authors declare that all data supporting the findings of the study are
572 available in this article and its Supplementary Information files, or from the corresponding author
573 upon request.
574
575 **Acknowledgements**. We thank members of the Berman and Bennett labs for stimulating
576 discussions throughout the work. We are grateful to G. Palmer, M. Lohse, O. Homann, A.
577 Johnson, R. Ben-Ami, T. White, D. Soll, D. McCallum, F. Odds, D. Sanglard, L. Cowen, P.T.
578 Magee, B. Cormack, P. Magwene, M. Kupiec, W. Fonzi, S. Noble, B.M. Vincent, S. Lindquist,
579 and A. Colombo for providing strains and P. Lipke, M. Fridman, R. BenAmi, N. Dror, A.
580 Selmecki, A.C. Gerstein and A. Forche for helpful comments on the manuscript. This work was
581 funded by European Research Council Advanced Award 340087 (RAPLODAPT) to JB, by
582 Fundação de Amparo a Pesquisa do Estado de São Paulo (FAPESP, Grant 2017/02203-7),
583 Brazil to ALC, by National Institutes of Health grant AI081704 to RJB and by a Brazil Initiative
584 Collaborative Grant from the Watson Institute to RJB and IVE.
585
586 **Author contributions**
587 IVE, RJB and JB designed the study; AR, IVE and AD collected the data; AR and IVE analyzed
588 the data, MB produced and analyzed data in Fig. 3a,d, SZ performed the experiment in
589 Supplementary Fig. 7g, ESS constructed mutant strains, NZ implemented and helped analyze

data in Fig. 2b, ALC provided clinical isolates and clinical input to the paper; AR, IVE, RJB and JB wrote the manuscript.

Figure legends

Figure 1. Measuring drug responses of *C. albicans* clinical isolates in disk diffusion assays (DDAs) and in liquid broth microdilution assays (BMDAs). (a) *diskImageR* analysis measures pixel intensity corresponding to cell density, along 72 radii every 5°. The average radius (RAD) represents the distance in mm corresponding to the point where 20%, 50% or 80% growth reduction occurs (light, medium, dark blue dots). The fraction of growth inside the zone of inhibition (FoG) is the area under the curve (red) at the RAD threshold, divided by the maximum area. (b) Range of FoG levels in 219 *C. albicans* clinical isolates. Red, blue and green lines estimate high, medium and low FoG levels, respectively. Unless otherwise specified, disk diffusion assays were performed using a single 25 µg FLC disk and analyzed after 48 h at 30°C. (c) Comparison of FoG_{20} and RAD_{20} for the 219 isolates. (d) Illustration of MIC and supra-MIC growth (SMG) calculations. MIC_{50} was calculated at 24 h as the FLC concentration at which 50% of the growth was inhibited, relative to growth in the absence of drug. SMG was calculated as the average growth per well above the MIC divided by the level of growth without drug. FLC was used in two-fold dilutions (0, 0.125 to 128 µg/ml). (e) Heatmaps illustrating OD_{600} levels for concentrations below the MIC (yellow bar) in cyan and above the MIC in yellow for the seven *C. albicans* isolates from Fig. 1c. Maps show OD_{600} values at 24 and 48 h. (f-g) Effect of incubation time on RAD/MIC and FoG/SMG values. *diskImageR* analysis (f) and corresponding MIC and SMG levels (g) measured at 24 and 48 h for strains as in (d). Of note, truly drug-resistant strains such as T101 (MIC = 64, Fig. 1e), the small zone of inhibition makes FoG measurements less accurate than SMG levels. (h) RAD is concentration-dependent and FoG is concentration-independent as measured with disks containing increasing concentrations

615 of FLC (25, 50 and 300 µg) for strain SC5314 shown for illustration (left); RAD (middle) and FoG
616 (right) levels for strains as listed.
617
618 **Figure 2.** Analysis of cells growing at supra-MIC concentrations. All tested strains, except for
619 T101 (MIC = 64 µg/ml), had FLC MIC values below 10 µg/ml. (a) FoG correlates with the
620 proportion of colonies that grow on 10 µg/ml FLC relative to growth on plates without drug. (b)
621 Microcolony analysis at supra-MIC concentrations of FLC (10 µg/ml). Symbols indicate cells
622 that have stopped dividing in the presence of drug over 24 h. On average, strain AM2 formed
623 fewer microcolonies than strain SC5314, but these were larger than those formed by SC5314.
624 Time lapse videos are available as Supplementary videos 1-4. (c,d) Growth rate analysis of
625 cells growing at supra-MIC FLC (10 µg/ml) during 0-5 h (c) and 10-15 h (d). (e) Schematic of
626 ScanLag analysis[75] that measures time of colony appearance (ToA), colony growth rate and
627 colony size using desktop scanners. (f) ToA on medium without drug (blue) or with 10 µg/ml
628 FLC (red) for resistant isolate T101, and isolates with different FoG levels. Graphs show the
629 number of colonies (y-axis) at each time point (x-axis). Additional isolates are included in
630 Supplementary Fig. 4. (g) Correlation between FoG_{20} and the difference (Δ) in the ToA of
631 colonies in the presence vs absence of FLC (ΔToA = ToA with FLC – ToA without FLC). (g)
632 Cells that grow within the zone of inhibition are viable, as seen by replica plating of disk diffusion
633 assays grown on casitone without FLC and incubated at 30°C for 48 h.
634
635 **Figure 3.** Uptake, efflux and steady state intracellular concentrations of FLC-Cy5. (a) Average
636 intracellular FLC-Cy5 uptake per cell. Uptake curves for 0-5 h and for steady state FLC-Cy5 per
637 cell at 24 h measured by flow cytometry. (b,c) Correlation between FoG_{20} and uptake rate of
638 FLC-Cy5 between 0.5-1.5h (b) and intracellular FLC-Cy5 at 24 h (c). (d) Intracellular FLC-Cy5
639 fluorescent intensity at 24 h for four strains with similar MIC and diverse FoG levels (left) and for
640 the resistant strain T101 (right) normalized for number of cells (n= 15863 for P87, 15075 of P78,

22406 for SC5314, 18186 of GC75); (e) The proportion of cells (%) with FLC-Cy5 levels at 24 h was divided into thirds: Low (391-422 A.U.), Mid (3912-34643 A.U.) and High ($3.5x10^4$-$3.14x10^5$ A.U.) (upper panel). Proportion of cells (%) with high (lower left panel) or mid (lower right panel) intracellular FLC-Cy5 concentration at 24 h vs FoG_{20} levels of the strains. (f) Efflux of Rhodamine 6G (R6G) normalized by culture density (OD_{600}). Efflux curves represent data from one (of two) experiments and the curves show fluorescence intensity recorded over 90 min and calculated as follows: Δ[FLC(with Glucose - without Glucose) – No drug(with Glucose - without Glucose)]. (g) Cartoon illustrates the steady state drug levels in cells with high to low FoG levels.

Figure 4. Adjuvant drugs significantly reduce FLC tolerance but not resistance and render FLC cidal. (a) Disk diffusion assays performed with 25 µg FLC on casitone plates supplemented with adjuvant drugs 20 µg/ml fluoxetine, 5 ng/ml aureobasidin A, 0.5 ng/ml rapamycin, 10 µg/ml fluphenazine, 12.5 ng/ml staurosporine, 0.25 µg/ml Tunicamycin, Hsp90 inhibitors (0.5 µg/ml geldanamycin and 0.5 µg/ml radicicol) and calcineurin inhibitors (0.5 µg/ml FK506 and 0.4 µg/ml cyclosporine A) shown for strain SC5314. (b) RAD and FoG levels performed on disk diffusion assays with FLC and adjuvants. (c) Effect of drug adjuvants and pathways inhibitors on the viability of cells growing inside the zone of inhibition. FLC disk diffusion assays of SC5314 without or with adjuvant were replica plated (after removal of the drug disk) onto casitone plates (without FLC or adjuvants) and incubated at 30°C for 48 h. (d,e) FLC disk diffusion assays performed using a series of mutants carrying deletions in gene encoding the calcineurin subunit Cnb1, the calcineurin responsive transcription factor Crz1, calcineurin regulators Rcn1 and Rcn2, MAP kinase Mkc1, vacuolar trafficking protein Vps21 (d), ergosterol biosynthesis regulator Upc2, and efflux pump regulators Tac1 and Mrr1 (e). These mutants as well as the *rcn1 crz1* double mutant were analyzed by *diskImageR,* and RAD and FoG levels are shown relative to the isogenic parental strains. All pictures in this figure are representative of two

667 biological replicates, asterisks denote significant differences relative to corresponding parental
668 strains, $P < 0.05$.
669
670 **Figure 5.** Combination therapy partially rescues systemic infection of *G. mellonella* by high
671 FoG *C. albicans* isolates. (a) *G. mellonella* larvae were injected with 3 x 10^5 yeast cells/larvae
672 followed by a second injection with either PBS, FLC alone or FLC and FNZ within 90 min after
673 the first injection. (b-d) Survival curves of larvae infected with SC5314, low FoG (c) and high
674 FoG (d) isogenic derivatives. Each curve represents a group of 24 larvae which were monitored
675 daily for survival for up to 14 days after infection. *P* values represent results of log-rank test
676 comparing different treatment conditions with significance values as follows: *, $P < 0.05$; **, $P <$
677 0.01; ***, $P < 0.001$.
678
679 **Figure 6**. FoG and SMG levels differ between persistent and non-persistent isolates. (a) *C.*
680 *albicans* isolates from bloodstream infections were either efficiently cleared by a single course
681 of FLC treatment (non-persistent) or persisted in the host despite multiple rounds of FLC
682 therapy. (b) FoG and RAD levels for drug-susceptible (S, n = 4) isolates SC5314, GC75,
683 P78042 and P87, resistant (R, n =1) isolate P60002[31], non-persistent isolates (NP, n = 7) and
684 the first patient isolate from each of the series of clinically persistent strains (P, n = 12). The
685 final isolate of the S03 series of persistent strains had become FLC-resistant (MIC > 128 µg/ml,
686 Supplementary Fig. 10a), therefore the penultimate isolate, which remained susceptible, was
687 used across analyses. Asterisks indicate significant differences between persistent and non-
688 persistent isolates (t-test, $P < 0.001$). (c) Broth microdilution assays showing MIC and SMG
689 levels at 24 and 48 h for the susceptible control strains, the non-persistent isolates as in (b) and
690 for both the initial and final isolates for each of the 12 clinically persistent series (S01-12). The
691 final isolate in S03 became FLC resistant (R), therefore the penultimate isolate in this series

692 was included as well. Asterisks indicate significant differences between persistent and non-
693 persistent isolates (t-test, $P < 0.001$).
694
695 **References**

696 1. CLSI. Performance Standards for Antimicrobial Susceptibility Testing. *CLSI supplement*
697 *M100* (2017).
698 2. Brauner, A., Fridman, O., Gefen, O. & Balaban, N.Q. Distinguishing between resistance,
699 tolerance and persistence to antibiotic treatment. *Nat Rev Microbiol* **14**, 320-30 (2016).
700 3. Coenye, T., De Vos, M., Vandenbosch, D. & Nelis, H. Factors influencing the trailing
701 endpoint observed in Candida albicans susceptibility testing using the CLSI procedure.
702 *Clin Microbiol Infect* **14**, 495-7 (2008).
703 4. Marcos-Zambrano, L.J., Escribano, P., Sanchez-Carrillo, C., Bouza, E. & Guinea, J.
704 Scope and frequency of fluconazole trailing assessed using EUCAST in invasive
705 Candida spp. isolates. *Med Mycol* **54**, 733-9 (2016).
706 5. Pfaller, M.A. & Diekema, D.J. Progress in antifungal susceptibility testing of Candida
707 spp. by use of Clinical and Laboratory Standards Institute broth microdilution methods,
708 2010 to 2012. *J Clin Microbiol* **50**, 2846-56 (2012).
709 6. Rex, J.H. & Pfaller, M.A. Has antifungal susceptibility testing come of age? *Clin Infect*
710 *Dis* **35**, 982-9 (2002).
711 7. Pfaller, M.A. *et al.* Wild-type MIC distributions and epidemiological cutoff values for
712 amphotericin B, flucytosine, and itraconazole and Candida spp. as determined by CLSI
713 broth microdilution. *J Clin Microbiol* **50**, 2040-6 (2012).
714 8. Alexander, B.D. *et al.* Increasing echinocandin resistance in Candida glabrata: clinical
715 failure correlates with presence of FKS mutations and elevated minimum inhibitory
716 concentrations. *Clin Infect Dis* **56**, 1724-32 (2013).

9. Doern, G.V. & Brecher, S.M. The Clinical Predictive Value (or Lack Thereof) of the Results of In Vitro Antimicrobial Susceptibility Tests. *Journal of Clinical Microbiology* **49**(2011).

10. Delarze, E. & Sanglard, D. Defining the frontiers between antifungal resistance, tolerance and the concept of persistence. *Drug Resist Updat* **23**, 12-19 (2015).

11. Balaban, N.Q., Gerdes, K., Lewis, K. & McKinney, J.D. A problem of persistence: still more questions than answers? *Nat Rev Microbiol* **11**, 587-91 (2013).

12. Da Matta, D.A. *et al.* Multilocus sequence typing of sequential Candida albicans isolates from patients with persistent or recurrent fungemia. *Med Mycol* **48**, 757-62 (2010).

13. Whaley, S.G. *et al.* Azole Antifungal Resistance in Candida albicans and Emerging Non-albicans Candida Species. *Front Microbiol* **7**, 2173 (2016).

14. Robbins, N., Caplan, T. & Cowen, L.E. Molecular Evolution of Antifungal Drug Resistance. *Annu Rev Microbiol* **71**, 753-775 (2017).

15. Cowen, L.E., Carpenter, A.E., Matangkasombut, O., Fink, G.R. & Lindquist, S. Genetic architecture of Hsp90-dependent drug resistance. *Eukaryot Cell* **5**, 2184-8 (2006).

16. Youngsaye, W. *et al.* Overcoming fluconazole resistance in Candida albicans clinical isolates with tetracyclic indoles. *Bioorg Med Chem Lett* **22**, 3362-5 (2012).

17. Blankenship, J.R., Steinbach, W.J., Perfect, J.R. & Heitman, J. Teaching old drugs new tricks: reincarnating immunosuppressants as antifungal drugs. *Curr Opin Investig Drugs* **4**, 192-9 (2003).

18. Kim, A. & Cunningham, K.W. A LAPF/phafin1-like protein regulates TORC1 and lysosomal membrane permeabilization in response to endoplasmic reticulum membrane stress. *Mol Biol Cell* **26**, 4631-45 (2015).

19. Fiori, A. & Van Dijck, P. Potent synergistic effect of doxycycline with fluconazole against Candida albicans is mediated by interference with iron homeostasis. *Antimicrob Agents Chemother* **56**, 3785-96 (2012).

20. Zhong, W., Jeffries, M.W. & Georgopapadakou, N.H. Inhibition of inositol phosphorylceramide synthase by aureobasidin A in Candida and Aspergillus species. *Antimicrob Agents Chemother* **44**, 651-3 (2000).

21. Gu, W., Guo, D., Zhang, L., Xu, D. & Sun, S. The Synergistic Effect of Azoles and Fluoxetine against Resistant Candida albicans Strains Is Attributed to Attenuating Fungal Virulence. *Antimicrob Agents Chemother* **60**, 6179-88 (2016).

22. Cruz, M.C. *et al.* Rapamycin and less immunosuppressive analogs are toxic to Candida albicans and Cryptococcus neoformans via FKBP12-dependent inhibition of TOR. *Antimicrob Agents Chemother* **45**, 3162-70 (2001).

23. Henry, K.W., Cruz, M.C., Katiyar, S.K. & Edlind, T.D. Antagonism of azole activity against Candida albicans following induction of multidrug resistance genes by selected antimicrobial agents. *Antimicrob Agents Chemother* **43**, 1968-74 (1999).

24. Robbins, N., Wright, G.D. & Cowen, L.E. Antifungal Drugs: The Current Armamentarium and Development of New Agents. *Microbiol Spectr* **4**(2016).

25. Geiler-Samerotte, K.A., Zhu, Y.O., Goulet, B.E., Hall, D.W. & Siegal, M.L. Selection Transforms the Landscape of Genetic Variation Interacting with Hsp90. *PLoS Biol* **14**, e2000465 (2016).

26. Jarosz, D.F. & Lindquist, S. Hsp90 and environmental stress transform the adaptive value of natural genetic variation. *Science* **330**, 1820-4 (2010).

27. Cowen, L.E. *et al.* Harnessing Hsp90 function as a powerful, broadly effective therapeutic strategy for fungal infectious disease. *Proc Natl Acad Sci U S A* **106**, 2818-23 (2009).

28. Sanglard, D., Ischer, F., Marchetti, O., Entenza, J. & Bille, J. Calcineurin A of Candida albicans: involvement in antifungal tolerance, cell morphogenesis and virulence. *Molecular microbiology* **48**, 959-976 (2003).

768 29. Coste, A.T., Karababa, M., Ischer, F., Bille, J. & Sanglard, D. TAC1, transcriptional
769 activator of CDR genes, is a new transcription factor involved in the regulation of
770 Candida albicans ABC transporters CDR1 and CDR2. *Eukaryot Cell* **3**, 1639-52 (2004).
771 30. Zhai, B., Wu, C., Wang, L., Sachs, M.S. & Lin, X. The antidepressant sertraline provides
772 a promising therapeutic option for neurotropic cryptococcal infections. *Antimicrob Agents*
773 *Chemother* **56**, 3758-66 (2012).
774 31. Pfaller, M.A. & Diekema, D.J. Epidemiology of invasive candidiasis: a persistent public
775 health problem. *Clinical microbiology reviews* **20**, 133-163 (2007).
776 32. Chapman, R.L. & Faix, R.G. Persistently positive cultures and outcome in invasive
777 neonatal candidiasis. *Pediatr Infect Dis J* **19**, 822-7 (2000).
778 33. Hammoud, M.S., Al-Taiar, A., Fouad, M., Raina, A. & Khan, Z. Persistent candidemia in
779 neonatal care units: risk factors and clinical significance. *Int J Infect Dis* **17**, e624-8
780 (2013).
781 34. Arendrup, M.C., Cuenca-Estrella, M., Lass-Florl, C., Hope, W. & Eucast, A. EUCAST
782 technical note on the EUCAST definitive document EDef 7.2: method for the
783 determination of broth dilution minimum inhibitory concentrations of antifungal agents for
784 yeasts EDef 7.2 (EUCAST-AFST). *Clin Microbiol Infect* **18**, E246-7 (2012).
785 35. Arthington-Skaggs, B.A. *et al.* Comparison of visual and spectrophotometric methods of
786 broth microdilution MIC end point determination and evaluation of a sterol quantitation
787 method for in vitro susceptibility testing of fluconazole and itraconazole against trailing
788 and nontrailing Candida isolates. *Antimicrob Agents Chemother* **46**, 2477-81 (2002).
789 36. Nicholas, R.O. & Kerridge, D. Correlation of inhibition of sterol synthesis with growth-
790 inhibitory action of imidazole antimycotics in Candida albicans. *J Antimicrob Chemother*
791 **23**, 7-19 (1989).

792 37. Rodriguez-Tudela, J.L. & Martinez-Suarez, J.V. Defining conditions for microbroth
793 antifungal susceptibility tests: influence of RPMI and RPMI-2% glucose on the selection
794 of endpoint criteria. *J Antimicrob Chemother* **35**, 739-49 (1995).
795 38. Luna-Tapia, A., Kerns, M.E., Eberle, K.E., Jursic, B.S. & Palmer, G.E. Trafficking
796 through the late endosome significantly impacts Candida albicans tolerance of the azole
797 antifungals. *Antimicrob Agents Chemother* **59**, 2410-20 (2015).
798 39. Whaley, S.G. *et al.* The RTA3 Gene, Encoding a Putative Lipid Translocase, Influences
799 the Susceptibility of Candida albicans to Fluconazole. *Antimicrob Agents Chemother* **60**,
800 6060-6 (2016).
801 40. Tscherner, M. *et al.* The Candida albicans Histone Acetyltransferase Hat1 Regulates
802 Stress Resistance and Virulence via Distinct Chromatin Assembly Pathways. *PLoS*
803 *Pathog* **11**, e1005218 (2015).
804 41. Xu, D., Cheng, J., Cao, C., Wang, L. & Jiang, L. Genetic interactions between Rch1 and
805 the high-affinity calcium influx system Cch1/Mid1/Ecm7 in the regulation of calcium
806 homeostasis, drug tolerance, hyphal development and virulence in Candida albicans.
807 *FEMS Yeast Res* **15**(2015).
808 42. Nagao, J. *et al.* Candida albicans Msi3p, a homolog of the Saccharomyces cerevisiae
809 Sse1p of the Hsp70 family, is involved in cell growth and fluconazole tolerance. *FEMS*
810 *Yeast Res* **12**, 728-37 (2012).
811 43. Rueda, C. *et al.* Evaluation of the possible influence of trailing and paradoxical effects on
812 the clinical outcome of patients with candidemia. *Clin Microbiol Infect* **23**, 49 e1-49 e8
813 (2017).
814 44. Chang, T.P. *et al.* Distribution and drug susceptibilities of Candida species causing
815 candidemia from a medical center in central Taiwan. *J Infect Chemother* **19**, 1065-71
816 (2013).

817 45. Rex, J.H. *et al.* Optimizing the correlation between results of testing in vitro and
818 therapeutic outcome in vivo for fluconazole by testing critical isolates in a murine model
819 of invasive candidiasis. *Antimicrob Agents Chemother* **42**, 129-34 (1998).
820 46. Arthington-Skaggs, B.A., Warnock, D.W. & Morrison, C.J. Quantitation of Candida
821 albicans ergosterol content improves the correlation between in vitro antifungal
822 susceptibility test results and in vivo outcome after fluconazole treatment in a murine
823 model of invasive candidiasis. *Antimicrob Agents Chemother* **44**, 2081-5 (2000).
824 47. Peters, B.M. *et al.* An Azole-Tolerant Endosomal Trafficking Mutant of Candida albicans
825 Is Susceptible to Azole Treatment in a Mouse Model of Vaginal Candidiasis. *Antimicrob*
826 *Agents Chemother* **61**(2017).
827 48. Revankar, S.G. *et al.* Interpretation of trailing endpoints in antifungal susceptibility testing
828 by the National Committee for Clinical Laboratory Standards method. *J Clin Microbiol* **36**,
829 153-6 (1998).
830 49. Agrawal, D., Patterson, T.F., Rinaldi, M.G. & Revankar, S.G. Trailing end-point
831 phenotype of Candida spp. in antifungal susceptibility testing to fluconazole is eliminated
832 by altering incubation temperature. *J Med Microbiol* **56**, 1003-4 (2007).
833 50. Marr, K.A., Rustad, T.R., Rex, J.H. & White, T.C. The trailing end point phenotype in
834 antifungal susceptibility testing is pH dependent. *Antimicrob Agents Chemother* **43**,
835 1383-6 (1999).
836 51. Singh, S.D. *et al.* Hsp90 governs echinocandin resistance in the pathogenic yeast
837 Candida albicans via calcineurin. *PLoS Pathog* **5**, e1000532 (2009).
838 52. Cannon, R.D. *et al.* Candida albicans drug resistance another way to cope with stress.
839 *Microbiology (Reading, England)* **153**, 3211-3217 (2007).
840 53. Karababa, M. *et al.* CRZ1, a target of the calcineurin pathway in Candida albicans.
841 *Molecular microbiology* **59**, 1429-1451 (2006).

54. LaFleur, M.D., Kumamoto, C.A. & Lewis, K. Candida albicans biofilms produce antifungal-tolerant persister cells. *Antimicrob Agents Chemother* **50**, 3839-46 (2006).

55. Onyewu, C., Wormley, F.L., Jr., Perfect, J.R. & Heitman, J. The calcineurin target, Crz1, functions in azole tolerance but is not required for virulence of Candida albicans. *Infection and immunity* **72**, 7330-7333 (2004).

56. Bonhomme, J. & d'Enfert, C. Candida albicans biofilms: building a heterogeneous, drug-tolerant environment. *Current opinion in microbiology* (2013).

57. Weil, T. *et al.* Adaptive Mistranslation Accelerates the Evolution of Fluconazole Resistance and Induces Major Genomic and Gene Expression Alterations in Candida albicans. *mSphere* **2**(2017).

58. Vincent, B.M. *et al.* A Fungal-Selective Cytochrome bc1 Inhibitor Impairs Virulence and Prevents the Evolution of Drug Resistance. *Cell Chem Biol* **23**, 978-991 (2016).

59. Hameed, S., Dhamgaye, S., Singh, A., Goswami, S.K. & Prasad, R. Calcineurin signaling and membrane lipid homeostasis regulates iron mediated multidrug resistance mechanisms in Candida albicans. *PLoS One* **6**, e18684 (2011).

60. Juvvadi, P.R., Lee, S.C., Heitman, J. & Steinbach, W.J. Calcineurin in fungal virulence and drug resistance: Prospects for harnessing targeted inhibition of calcineurin for an antifungal therapeutic approach. *Virulence* **8**, 186-197 (2017).

61. Cowen, L.E. & Lindquist, S. Hsp90 potentiates the rapid evolution of new traits: drug resistance in diverse fungi. *Science* **309**, 2185-9 (2005).

62. Tavanti, A., Gow, N.A., Senesi, S., Maiden, M.C. & Odds, F.C. Optimization and validation of multilocus sequence typing for Candida albicans. *J Clin Microbiol* **41**, 3765-76 (2003).

63. MacCallum, D.M. *et al.* Property differences among the four major Candida albicans strain clades. *Eukaryot Cell* **8**, 373-87 (2009).

867 64. McManus, B.A. & Coleman, D.C. Molecular epidemiology, phylogeny and evolution of
868 Candida albicans. *Infect Genet Evol* **21**, 166-78 (2014).
869 65. Gerstein, A.C., Rosenberg, A., Hecht, I. & Berman, J. diskImageR: quantification of
870 resistance and tolerance to antimicrobial drugs using disk diffusion assays. *Microbiology*
871 **162**, 1059-68 (2016).
872 66. Sanglard, D., Ischer, F., Marchetti, O., Entenza, J. & Bille, J. Calcineurin A of Candida
873 albicans: involvement in antifungal tolerance, cell morphogenesis and virulence. *Mol*
874 *Microbiol* **48**, 959-76 (2003).
875 67. Marchetti, O., Moreillon, P., Glauser, M.P., Bille, J. & Sanglard, D. Potent synergism of
876 the combination of fluconazole and cyclosporine in Candida albicans. *Antimicrob Agents*
877 *Chemother* **44**, 2373-81 (2000).
878 68. Alp, S., Sancak, B., Hascelik, G. & Arikan, S. Influence of different susceptibility testing
879 methods and media on determination of the relevant fluconazole minimum inhibitory
880 concentrations for heavy trailing Candida isolates with low-high phenotype. *Mycoses* **53**,
881 475-80 (2010).
882 69. Vandenbossche, I., Vaneechoutte, M., Vandevenne, M., De Baere, T. & Verschraegen,
883 G. Susceptibility testing of fluconazole by the NCCLS broth macrodilution method, E-
884 test, and disk diffusion for application in the routine laboratory. *J Clin Microbiol* **40**, 918-
885 21 (2002).
886 70. Pfaller, M.A. *et al.* Comparison of results of fluconazole disk diffusion testing for Candida
887 species with results from a central reference laboratory in the ARTEMIS global
888 antifungal surveillance program. *J Clin Microbiol* **42**, 3607-12 (2004).
889 71. Zomorodian, K. *et al.* In Vitro Susceptibility and Trailing Growth Effect of Clinical Isolates
890 of Candida Species to Azole Drugs. *Jundishapur J Microbiol* **9**, e28666 (2016).
891 72. Levy, S.F., Ziv, N. & Siegal, M.L. Bet hedging in yeast by heterogeneous, age-correlated
892 expression of a stress protectant. *PLoS Biol* **10**, e1001325 (2012).

73. Harrison, B.D. *et al.* A tetraploid intermediate precedes aneuploid formation in yeasts exposed to fluconazole. *PLoS Biol* **12**, e1001815 (2014).

74. Levin-Reisman, I., Fridman, O. & Balaban, N.Q. ScanLag: high-throughput quantification of colony growth and lag time. *J Vis Exp* (2014).

75. Levin-Reisman, I. & Balaban, N.Q. Quantitative Measurements of Type I and Type II Persisters Using ScanLag. *Methods Mol Biol* **1333**, 75-81 (2016).

76. Fridman, O., Goldberg, A., Ronin, I., Shoresh, N. & Balaban, N.Q. Optimization of lag time underlies antibiotic tolerance in evolved bacterial populations. *Nature* **513**, 418-21 (2014).

77. Balaban, N.Q., Merrin, J., Chait, R., Kowalik, L. & Leibler, S. Bacterial persistence as a phenotypic switch. *Science* **305**, 1622-5 (2004).

78. Alby, K. & Bennett, R.J. Stress-induced phenotypic switching in Candida albicans. *Molecular biology of the cell* **20**, 3178-3191 (2009).

79. Bensen, E.S., Clemente-Blanco, A., Finley, K.R., Correa-Bordes, J. & Berman, J. The mitotic cyclins Clb2p and Clb4p affect morphogenesis in Candida albicans. *Mol Biol Cell* **16**, 3387-400 (2005).

80. Bull, J.J., Vegge, C.S., Schmerer, M., Chaudhry, W.N. & Levin, B.R. Phenotypic resistance and the dynamics of bacterial escape from phage control. *PLoS One* **9**, e94690 (2014).

81. Benhamou, R.I. *et al.* Real-Time Imaging of the Azole Class of Antifungal Drugs in Live Candida Cells. *ACS Chem Biol* **12**, 1769-1777 (2017).

82. Ben-Ami, R. *et al.* Heteroresistance to Fluconazole Is a Continuously Distributed Phenotype among Candida glabrata Clinical Strains Associated with In Vivo Persistence. *MBio* **7**(2016).

83. Veri, A. & Cowen, L.E. Progress and prospects for targeting Hsp90 to treat fungal infections. *Parasitology* **141**, 1127-1137 (2014).

84. Shrestha, S.K., Fosso, M.Y. & Garneau-Tsodikova, S. A combination approach to treating fungal infections. *Sci Rep* **5**, 17070 (2015).

85. Chaturvedi, V. *et al.* Multilaboratory testing of two-drug combinations of antifungals against Candida albicans, Candida glabrata, and Candida parapsilosis. *Antimicrob Agents Chemother* **55**, 1543-8 (2011).

86. Kaneko, Y., Ohno, H., Imamura, Y., Kohno, S. & Miyazaki, Y. The effects of an hsp90 inhibitor on the paradoxical effect. *Jpn J Infect Dis* **62**, 392-3 (2009).

87. Uppuluri, P., Nett, J., Heitman, J. & Andes, D. Synergistic effect of calcineurin inhibitors and fluconazole against Candida albicans biofilms. *Antimicrob Agents Chemother* **52**, 1127-32 (2008).

88. Cruz, M.C. *et al.* Calcineurin is essential for survival during membrane stress in Candida albicans. *EMBO J* **21**, 546-59 (2002).

89. Onyewu, C., Blankenship, J.R., Del Poeta, M. & Heitman, J. Ergosterol biosynthesis inhibitors become fungicidal when combined with calcineurin inhibitors against Candida albicans, Candida glabrata, and Candida krusei. *Antimicrob Agents Chemother* **47**, 956-64 (2003).

90. LaFayette, S.L. *et al.* PKC signaling regulates drug resistance of the fungal pathogen Candida albicans via circuitry comprised of Mkc1, calcineurin, and Hsp90. *PLoS Pathog* **6**, e1001069 (2010).

91. Chen, S.C., Lewis, R.E. & Kontoyiannis, D.P. Direct effects of non-antifungal agents used in cancer chemotherapy and organ transplantation on the development and virulence of Candida and Aspergillus species. *Virulence* **2**, 280-95 (2011).

92. Lehle, L. & Tanner, W. The specific site of tunicamycin inhibition in the formation of dolichol-bound N-acetylglucosamine derivatives. *FEBS Lett* **72**, 167-70 (1976).

943 93. Stefan, C.P. & Cunningham, K.W. Kch1 family proteins mediate essential responses to
944 endoplasmic reticulum stresses in the yeasts Saccharomyces cerevisiae and Candida
945 albicans. *J Biol Chem* **288**, 34861-70 (2013).
946 94. Tkacz, J.S. & Lampen, O. Tunicamycin inhibition of polyisoprenyl N-acetylglucosaminyl
947 pyrophosphate formation in calf-liver microsomes. *Biochem Biophys Res Commun* **65**,
948 248-57 (1975).
949 95. Cyert, M.S. Genetic analysis of calmodulin and its targets in Saccharomyces cerevisiae.
950 *Annu Rev Genet* **35**, 647-72 (2001).
951 96. White, T.C. Increased mRNA levels of ERG16, CDR, and MDR1 correlate with increases
952 in azole resistance in Candida albicans isolates from a patient infected with human
953 immunodeficiency virus. *Antimicrob Agents Chemother* **41**, 1482-7 (1997).
954 97. Redding, S. *et al.* Resistance of Candida albicans to fluconazole during treatment of
955 oropharyngeal candidiasis in a patient with AIDS: documentation by in vitro susceptibility
956 testing and DNA subtype analysis. *Clin Infect Dis* **18**, 240-2 (1994).
957 98. CLSI. Reference method for broth dilution antifungal susceptibility testing of yeasts; 4th
958 Informational Supplement. *CLSI document M27-S4. Wayne: Clinical and Laboratory*
959 *Standards Institute; .* (2012).
960 99. Marchetti, O. *et al.* Fluconazole plus cyclosporine: a fungicidal combination effective
961 against experimental endocarditis due to Candida albicans. *Antimicrob Agents*
962 *Chemother* **44**, 2932-8 (2000).
963 100. Cowen, L.E. & Steinbach, W.J. Stress, drugs, and evolution: the role of cellular signaling
964 in fungal drug resistance. *Eukaryotic cell* **7**, 747-764 (2008).
965 101. Reedy, J.L., Filler, S.G. & Heitman, J. Elucidating the Candida albicans calcineurin
966 signaling cascade controlling stress response and virulence. *Fungal Genet Biol* **47**, 107-
967 16 (2010).

968 102. Edlind, T., Smith, L., Henry, K., Katiyar, S. & Nickels, J. Antifungal activity in
969 Saccharomyces cerevisiae is modulated by calcium signalling. *Mol Microbiol* **46**, 257-68
970 (2002).
971 103. Colombo, A.L., de Almeida Junior, J.N., Slavin, M.A., Chen, S.C. & Sorrell, T.C. Candida
972 and invasive mould diseases in non-neutropenic critically ill patients and patients with
973 haematological cancer. *Lancet Infect Dis* (2017).
974 104. Nucci, M. *et al.* Epidemiology of candidemia in Latin America: a laboratory-based survey.
975 *PLoS One* **8**, e59373 (2013).
976 105. Reboli, A.C. *et al.* Anidulafungin versus fluconazole for invasive candidiasis. *N Engl J*
977 *Med* **356**, 2472-82 (2007).
978 106. Andes, D.R. *et al.* Impact of treatment strategy on outcomes in patients with candidemia
979 and other forms of invasive candidiasis: a patient-level quantitative review of randomized
980 trials. *Clin Infect Dis* **54**, 1110-22 (2012).
981 107. Braga-Silva, L.A. *et al.* Trailing end-point phenotype antibiotic-sensitive strains of
982 Candida albicans produce different amounts of aspartyl peptidases. *Braz J Med Biol Res*
983 **42**, 765-70 (2009).
984 108. Shapiro, R.S., Zaas, A.K., Betancourt-Quiroz, M., Perfect, J.R. & Cowen, L.E. The
985 Hsp90 co-chaperone Sgt1 governs Candida albicans morphogenesis and drug
986 resistance. *PLoS One* **7**, e44734 (2012).
987 109. Prasad, R., Rawal, M.K. & Shah, A.H. Candida Efflux ATPases and Antiporters in
988 Clinical Drug Resistance. *Adv Exp Med Biol* **892**, 351-376 (2016).
989 110. Nim, S. *et al.* Overcoming Multidrug Resistance in Candida albicans: Macrocyclic
990 Diterpenes from Euphorbia Species as Potent Inhibitors of Drug Efflux Pumps. *Planta*
991 *Med* **82**, 1180-5 (2016).
992 111. Holmes, A.R. *et al.* Targeting efflux pumps to overcome antifungal drug resistance.
993 *Future Med Chem* **8**, 1485-501 (2016).

994 112. Cowen, L.E., Sanglard, D., Howard, S.J., Rogers, P.D. & Perlin, D.S. Mechanisms of
995 Antifungal Drug Resistance. *Cold Spring Harbor Perspectives in Medicine* **5**(2015).
996 113. Prasad, R. & Rawal, M.K. Efflux pump proteins in antifungal resistance. *Front Pharmacol*
997 **5**, 202 (2014).
998 114. Schubert, S. *et al.* Regulation of efflux pump expression and drug resistance by the
999 transcription factors Mrr1, Upc2, and Cap1 in Candida albicans. *Antimicrob Agents*
1000 *Chemother* **55**, 2212-23 (2011).
1001 115. Morschhauser, J. *et al.* The transcription factor Mrr1p controls expression of the MDR1
1002 efflux pump and mediates multidrug resistance in Candida albicans. *PLoS Pathog* **3**,
1003 e164 (2007).
1004 116. Prasad, R., Gaur, N.A., Gaur, M. & Komath, S.S. Efflux pumps in drug resistance of
1005 Candida. *Infect Disord Drug Targets* **6**, 69-83 (2006).
1006 117. Akins, R.A. An update on antifungal targets and mechanisms of resistance in Candida
1007 albicans. *Med Mycol* **43**, 285-318 (2005).
1008 118. Maesaki, S., Marichal, P., Vanden Bossche, H., Sanglard, D. & Kohno, S. Rhodamine
1009 6G efflux for the detection of CDR1-overexpressing azole-resistant Candida albicans
1010 strains. *J Antimicrob Chemother* **44**, 27-31 (1999).
1011 119. Vasicek, E.M. *et al.* Disruption of the transcriptional regulator Cas5 results in enhanced
1012 killing of Candida albicans by Fluconazole. *Antimicrob Agents Chemother* **58**, 6807-18
1013 (2014).
1014 120. Liu, S. *et al.* Synergistic Effect of Fluconazole and Calcium Channel Blockers against
1015 Resistant Candida albicans. *PLoS One* **11**, e0150859 (2016).
1016 121. Epp, E. *et al.* Reverse genetics in Candida albicans predicts ARF cycling is essential for
1017 drug resistance and virulence. *PLoS Pathog* **6**, e1000753 (2010).

1018 122. Cardenas, M.E., Sanfridson, A., Cutler, N.S. & Heitman, J. Signal-transduction cascades
1019 as targets for therapeutic intervention by natural products. *Trends Biotechnol* **16**, 427-33
1020 (1998).
1021 123. Elicharova, H. & Sychrova, H. Fluconazole treatment hyperpolarizes the plasma
1022 membrane of Candida cells. *Med Mycol* **51**, 785-94 (2013).
1023 124. Kohli, A., Smriti, Mukhopadhyay, K., Rattan, A. & Prasad, R. In vitro low-level resistance
1024 to azoles in Candida albicans is associated with changes in membrane lipid fluidity and
1025 asymmetry. *Antimicrob Agents Chemother* **46**, 1046-52 (2002).
1026 125. Sorgo, A.G. *et al.* Effects of fluconazole on the secretome, the wall proteome, and wall
1027 integrity of the clinical fungus Candida albicans. *Eukaryot Cell* **10**, 1071-81 (2011).
1028 126. Saarikangas, J. & Barral, Y. Protein aggregation as a mechanism of adaptive cellular
1029 responses. *Curr Genet* **62**, 711-724 (2016).
1030 127. Corona, F. & Martinez, J.L. Phenotypic Resistance to Antibiotics. *Antibiotics (Basel)* **2**,
1031 237-55 (2013).
1032 128. Nussbaum, J.C. *et al.* Combination flucytosine and high-dose fluconazole compared with
1033 fluconazole monotherapy for the treatment of cryptococcal meningitis: a randomized trial
1034 in Malawi. *Clin Infect Dis* **50**, 338-44 (2010).
1035 129. Colombo, A.L. *et al.* Prognostic factors and historical trends in the epidemiology of
1036 candidemia in critically ill patients: an analysis of five multicenter studies sequentially
1037 conducted over a 9-year period. *Intensive Care Med* **40**, 1489-98 (2014).
1038 130. CLSI. Method for Antifungal Disk Diffusion Susceptiplity Testing of Yeasts; Approved
1039 Guideline-Second Edition. *CLSI document M27-S4. Wayne: Clinical and Laboratory*
1040 *Standards Institute* (2009).
1041 131. Diezmann, S., Michaut, M., Shapiro, R.S., Bader, G.D. & Cowen, L.E. Mapping the
1042 Hsp90 genetic interaction network in Candida albicans reveals environmental
1043 contingency and rewired circuitry. *PLoS Genet* **8**, e1002562 (2012).

1044 132. Vale-Silva, L.A. *et al.* Azole resistance by loss of function of the sterol Delta(5),(6)-
1045 desaturase gene (ERG3) in Candida albicans does not necessarily decrease virulence.
1046 *Antimicrob Agents Chemother* **56**, 1960-8 (2012).
1047 133. Li, D.D. *et al.* Using Galleria mellonella-Candida albicans infection model to evaluate
1048 antifungal agents. *Biol Pharm Bull* **36**, 1482-7 (2013).
1049 134. Ziv, N., Siegal, M.L. & Gresham, D. Genetic and nongenetic determinants of cell growth
1050 variation assessed by high-throughput microscopy. *Mol Biol Evol* **30**, 2568-78 (2013).
1051
1052

Figure 1

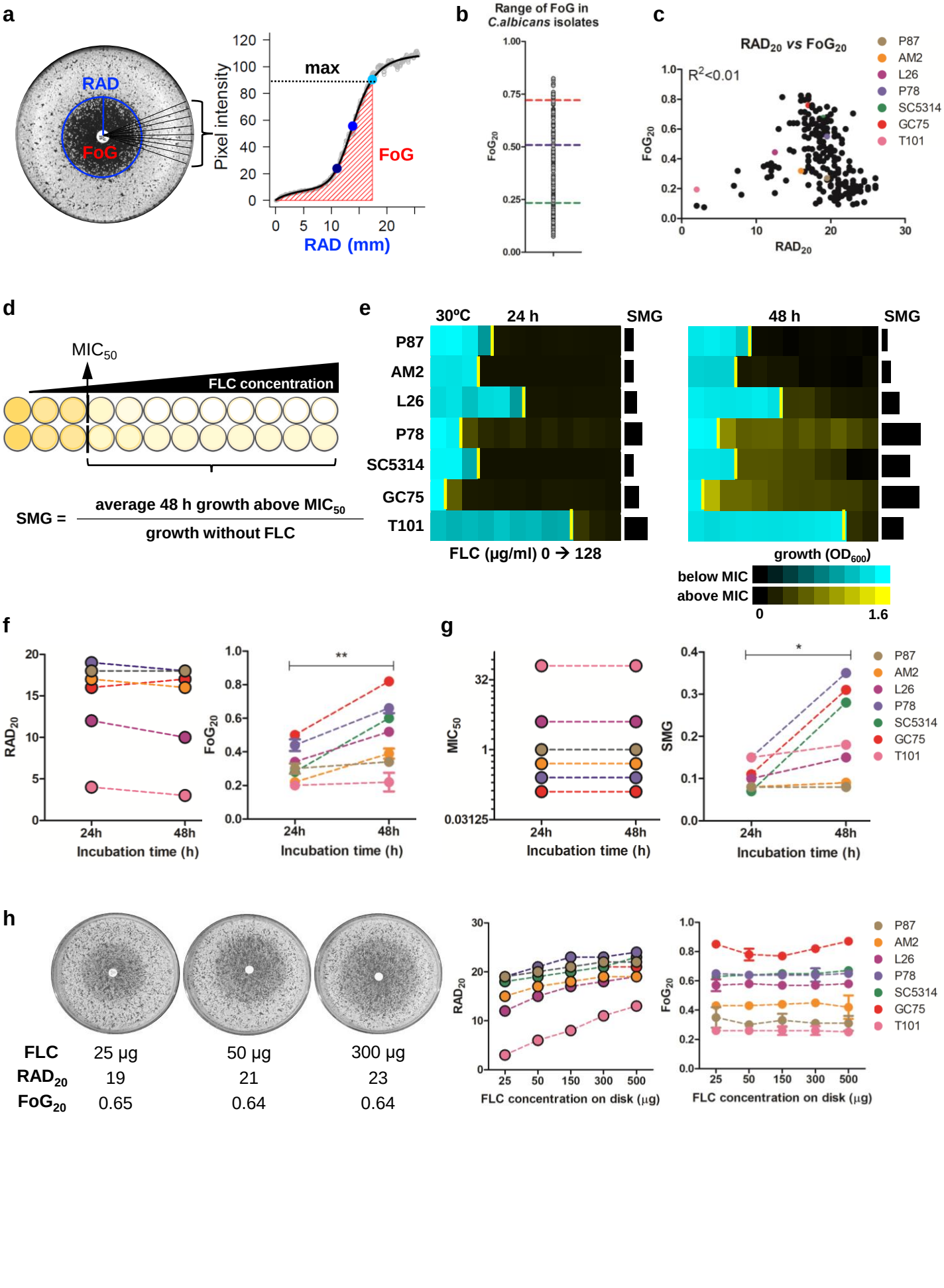

Figure 2

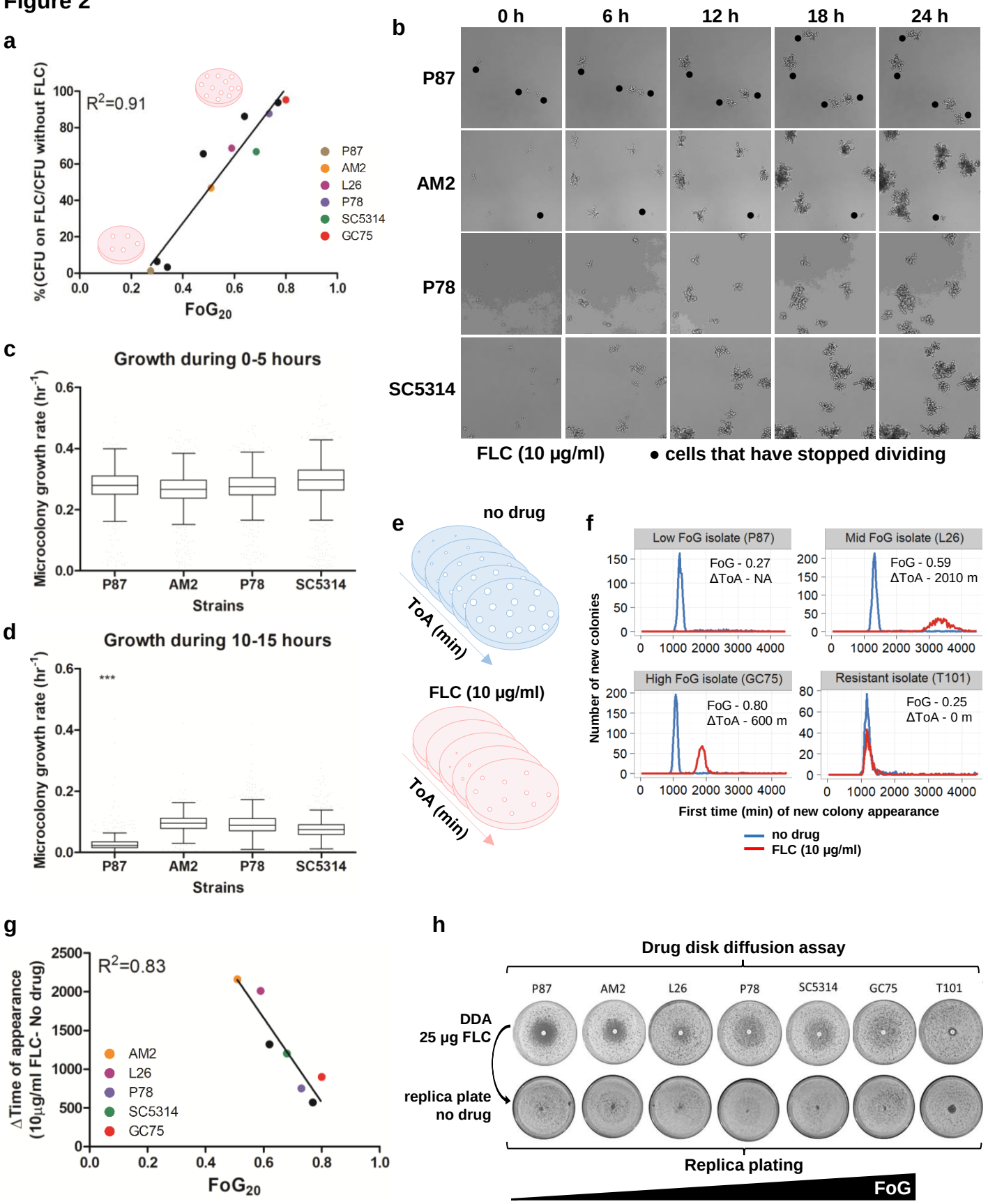

Figure 3

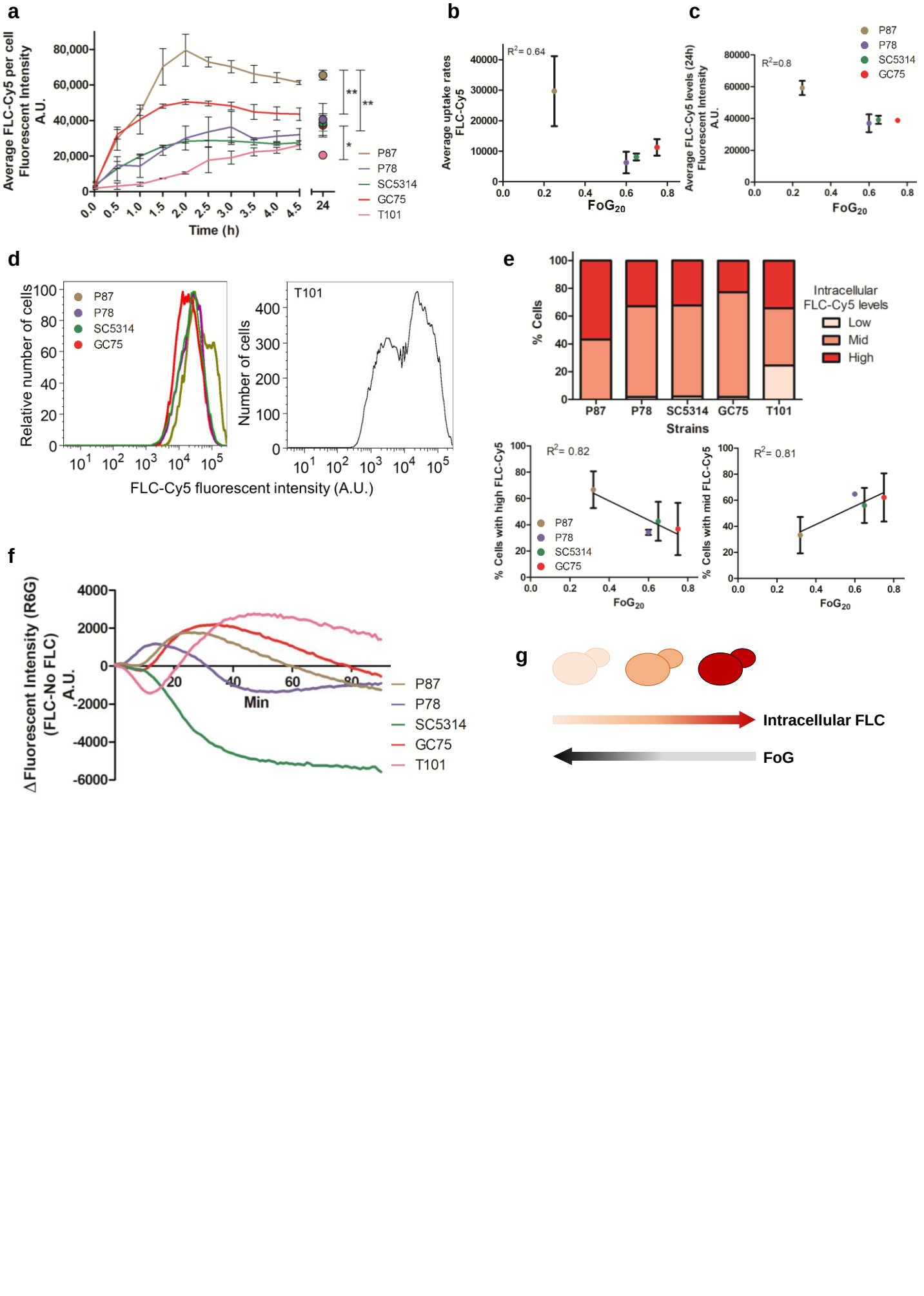

Figure 4

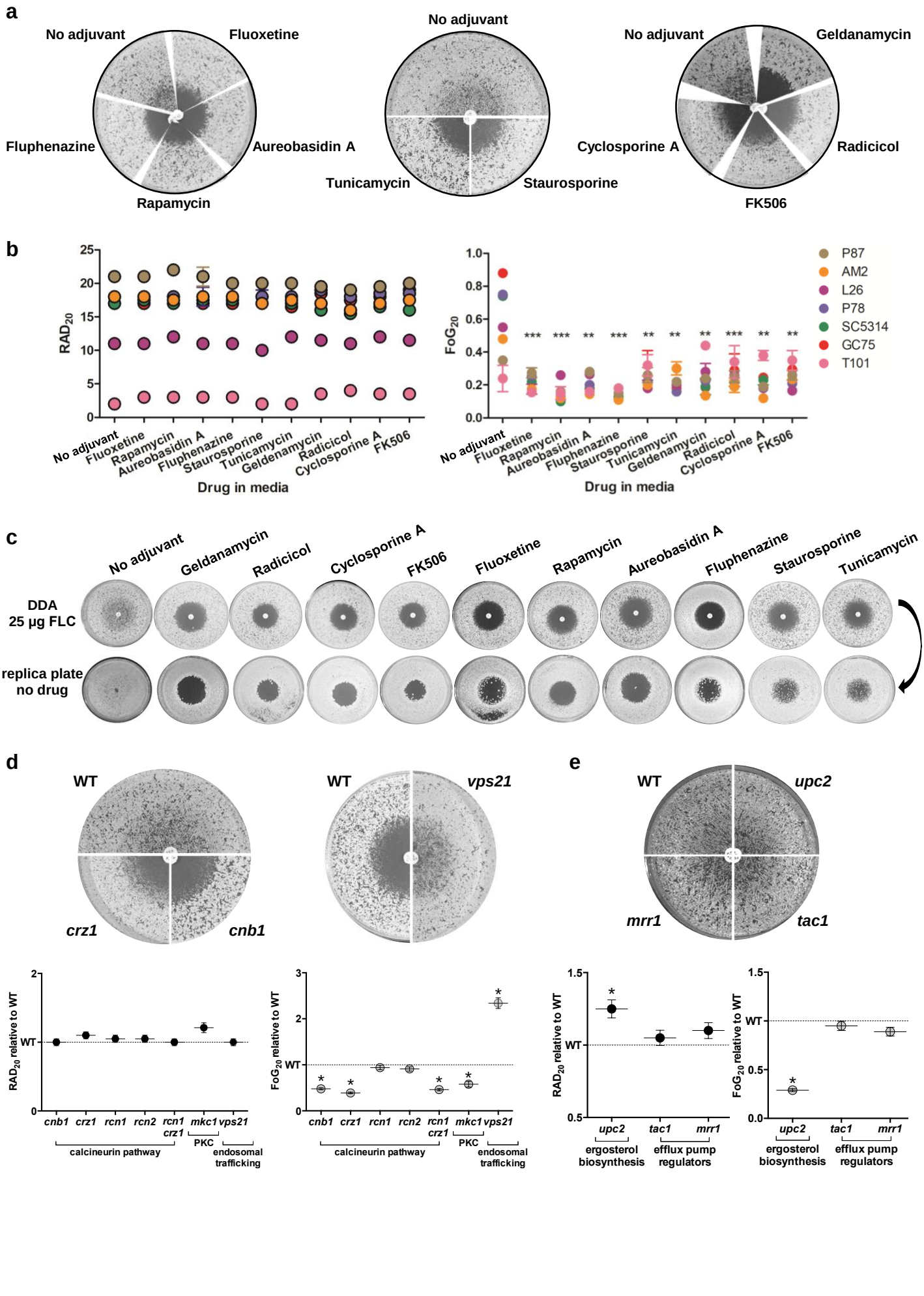

Figure 5

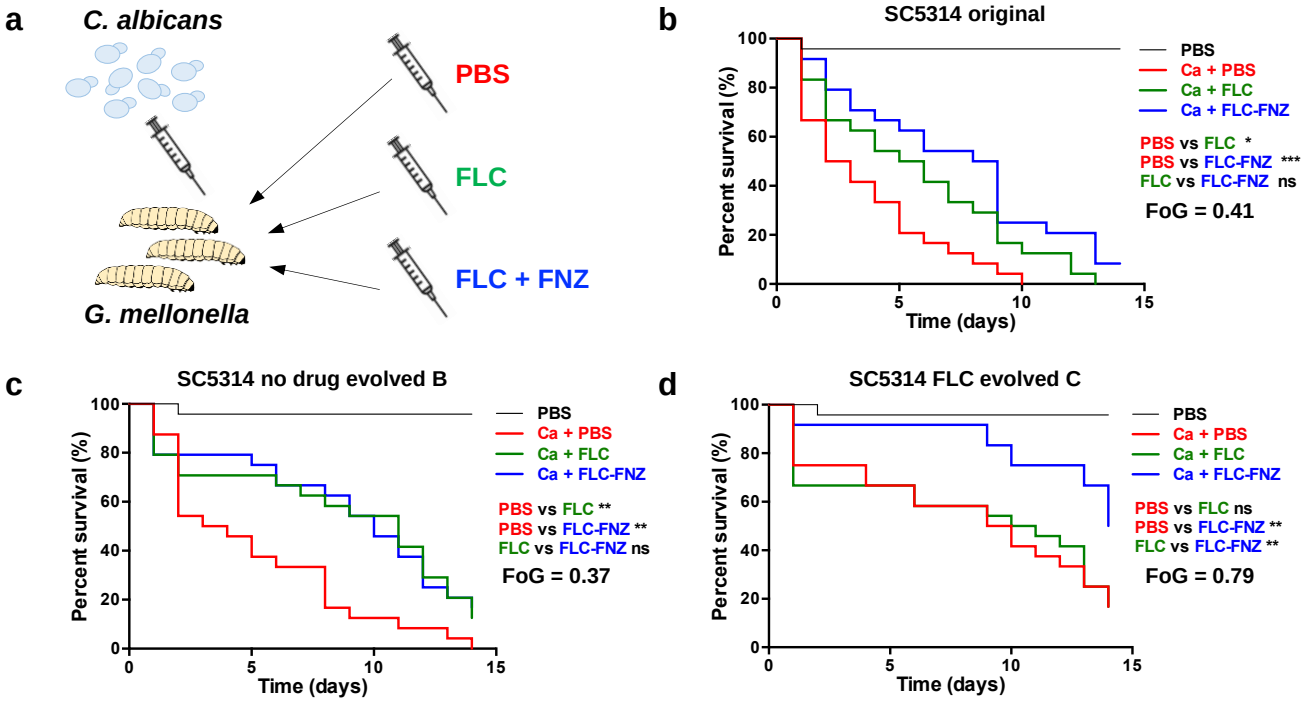

Figure 6